Journal of Superconductivity, Vol. 3, No. 3, 1990

Magnetic Penetration Depth Measurements with the Microstrip Resonator Technique

S. M. Anlage,[1] B. W. Langley,[1] H. J. Snortland,[1] C. B. Eom,[1] T. H. Geballe,[1] and M. R. Beasley[1]

Received 27 March 1990

The microstrip resonator technique is a convenient way to sensitively measure the temperature dependence of the magnetic penetration depth $\lambda(T)$ in superconducting thin films. Because the method relies on measuring the resonant frequency of a high-Q transmission line resonator at microwave frequencies, one can very precisely measure small changes in $\lambda(T)$. This technique is applied to studying the low-temperature dependence of $\lambda(T)$, since that is in principle a measure of the low-lying pair-breaking excitations of the superconductor. We find that the penetration depth in niobium films is consistent with the predictions of weak coupled BCS theory. The low-temperature dependence of $\lambda(T)$ in c-axis $YBa_2Cu_3O_{7-\delta}$ films can be interpreted as either a weak exponential or as a power law. In addition, the measured value of $\lambda(0)$ is found to be strongly dependent on the form of the temperature dependence for $\lambda(T)$ used in fitting the data. Best fits over the entire temperature range are obtained with a BCS temperature dependence having values for $2\Delta(0)/k_BT_c$ strictly less than 3.5, consistent with our measurements of the temperature dependence of $\lambda(T)$ at low temperatures in $YBa_2Cu_3O_{7-\delta}$.

KEY WORDS: High-temperature superconductivity; magnetic penetration depth; microwave surface impedance.

1. INTRODUCTION

In response to an external magnetic field, a superconductor generates currents near its surface to shield out the applied field. The characteristic depth to which the shielding currents flow is the magnetic penetration depth, λ. This penetration depth depends on temperature, starting from a finite value at low temperature and increasing monotonically as T approaches T_c.

The penetration depth is sensitive to the properties of the superconductor near its surface, or in a film of thickness $t \approx \lambda$, to the entire film. The temperature dependence is also sensitive to the nature of the quasiparticle excitation spectrum, since as temperature increases it is sensitive to how the superconducting electron density is depleted by thermal excitations.

2. MAGNETIC PENETRATION DEPTH MEASUREMENTS

2.1. Principle of the Measurement

A sensitive way to measure the penetration depth of thin films is to take advantage of the fact that the surface inductance of these films is strongly dependent on the magnitude of the penetration depth. The inductance of a superconducting thin film has two components, one related to geometry and the other related to the kinetic energy of the charge carriers. The geometrical inductance is associated with the magnetic fields generated by a current in the thin film, and depends on the geometry of the thin film and the distance to nearby conductors. The kinetic inductance

[1]Department of Applied Physics, Stanford University, Stanford, California 94305.

0896-1107/90/0900-0311$06.00/0

is associated with the kinetic inertia of the charge carriers, and can be made quite large compared to the geometrical inductance for films thinner than the penetration depth. Since the kinetic inductance is strongly dependent on the magnitude of the penetration depth of the thin film, the total inductance of the superconducting film can be used as a sensitive measure of the penetration depth itself.

Since a direct measurement of the thin film inductance is difficult, it is more practical to make the inductor part of an electrical circuit and measure some property of that circuit which is sensitive to the inductance. We choose to make a superconducting transmission line since the phase velocity of a signal propagating along this line depends on the surface inductance.

Consider the superconducting microstrip as a particular realization of a transmission line (see Fig. 1a). In the one-dimensional limit (line width $\gg$ dielectric thickness), the series inductance and shunt capacitance (both per unit line length) of the microstrip are given by [1]

$$L=\frac{\mu_0}{w}\left\{d+2\lambda\coth\left(\frac{t}{\lambda}\right)\right\}$$

$$C=\varepsilon_0\varepsilon_r\frac{2}{d}$$

where t and d are the film and dielectric thicknesses, w is the strip width, and ε_r is the relative dielectric constant. The phase velocity for a signal propagating on a lossless transmission line is [1]

$$v_{\mathrm{ph}}(T)=\frac{1}{\sqrt{LC}}=\frac{c/\sqrt{\varepsilon_r}}{\sqrt{1+\dfrac{2\lambda(T)\coth\left(t/\lambda(T)\right)}{d}}} \tag{1}$$

Clearly, if one can measure $v_{\mathrm{ph}}(T)$, Eq. (1) can be inverted and solved for $\lambda(T)$ uniquely for a given t, d, and ε_r.

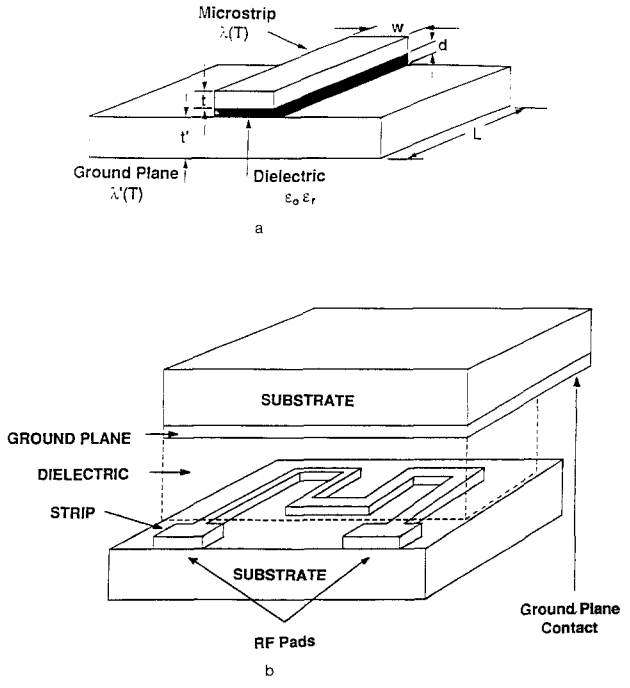

Fig. 1. (a) The microstrip transmission line, consisting of ground plane and microstrip films of thickness t and a dielectric of thickness d and relative dielectric constant ε_r. The strip film is of width w. (b) A flip-chip microstrip transmission line resonator consisting of an unpatterned ground plane film, a patterned strip film, and a dielectric material in between.

2.2. Two-Dimensional and Finite-Attenuation Corrections

For most of the superconducting microstrip lines that we have studied, the condition of one-dimensional behavior is not well satisfied. Typical lines have a width of 15–25 μm and a dielectric thickness of 12–25 μm, so that we rarely have microstrip lines for which the line width is much greater than the dielectric thickness. Two-dimensional effects, such as field fringing and asymmetric contributions to the total inductance from the strip and ground plane conductors, must be taken into account for these lines. Nevertheless, the above equations can be used in this case with only slight modification. The relative dielectric constant (ε_r) must be replaced by an effective relative dielectric constant ($\varepsilon_{\mathrm{eff}}$), which takes the multiple dielectric system into account, and a fringing field factor (k) must be introduced. The total inductance also has an additional term that reflects the ground/strip asymmetry. Chang [2] used a conformal mapping technique to obtain the two-dimensional superconducting microstrip line inductance,

$$L=\frac{\mu_0}{wk}\left(d+2\lambda\coth\left(\frac{t}{\lambda}\right)+g_c\lambda\,\mathrm{csch}\left(\frac{t}{\lambda}\right)\right)$$

The fringing field factor k is a function of the line width, dielectric thickness, and film thickness. The conductor asymmetry factor g_c is also a function of the microstrip geometry. With these corrections, the

capacitance and phase velocity become

$$C = k\varepsilon_{\text{eff}}\varepsilon_0 \frac{w}{d}$$

$$v_{\text{ph}} = \frac{c/\sqrt{\varepsilon_{\text{eff}}}}{\sqrt{1+\frac{2\lambda}{d}\coth\left(\frac{t}{\lambda}\right)+\frac{g_c\lambda}{d}\operatorname{csch}\left(\frac{t}{\lambda}\right)}}$$

We have also investigated the effect of finite attenuation on the phase velocity. We find that for typical measurement frequencies (1-10 GHz) and $T<0.99\ T_c$, the effect of finite attenuation on the phase velocity of a superconducting transmission line is negligible. A more detailed discussion of these corrections will be published later [3].

2.3. Practical Aspects of the Measurement

A direct measurement of the phase velocity on a laboratory length scale transmission line is not very accurate. It is better to perform the measurement in the frequency domain where frequencies can be measured quite accurately with readily available equipment. This can be accomplished by terminating the transmission line with a large impedance mismatch at both ends and so as to form a transmission line resonator. The length of the resonator, L, determines the resonant frequency, which is simply related to the phase velocity as $v_{\text{ph}} = 2Lf_n/n$, where f_n is the nth harmonic frequency. We have chosen $L \approx 4$ cm, so the resonant frequencies are in the gigahertz range. Microwave sources with internal frequency stability of one part in 10^9 are commercially available, making microstrip resonator measurements of $\lambda(T)$ potentially very sensitive.

In practice the transmission line resonators are realized in two ways:

1. *Flip Chip Geometry.* In this case, one film is patterned with a long meandering line and terminated with coupling pads, while the other film is left unpatterned and forms the ground plane (see Fig. 1b). The two films are clamped together, face to face, with a dielectric material in between. We typically use Mylar or Teflon sheets of 1/2 or 1 mil thickness, or sapphire wafers of 40-50 μm thickness. This results in a multiple dielectric medium which complicates the calculation of ε_{eff}. However, the results of the $\lambda(T)$ measurements are independent of the dielectrics chosen.
2. *Integrated Microstrip Geometry.* In this case, the ground plane, dielectric, and strip films are deposited sequentially onto the same substrate. These integrated transmission lines have been made with Nb superconducting films with polyimide as the dielectric.

3. SUPERCONDUCTING FILMS

Niobium films have been prepared by electron-beam evaporation [4]. The films were deposited on R-plane sapphire and are (100) textured as seen in X-ray diffraction. The resistive T_c is approximately 9.2 K before patterning, and the residual resistivity ratio is approximately 25 for 500-Å thick films.

In-situ films of $YBa_2Cu_3O_{7-\delta}$ have been prepared at Stanford by off-axis sputtering [5] and reactive electron-beam coevaporation [6]. These films show high critical current densities [7] and good RF properties [8]. Resistive transition temperatures are in the range of 85-90 K.

All of the $YBa_2Cu_3O_{7-\delta}$ films are c-axis normal oriented, meaning that the shielding currents used to measure the penetration depth flow in the ab-plane.

4. MEASUREMENTS

4.1. Low-Temperature $\lambda(T)$ Dependence

We wish to extract the temperature dependence of $\lambda(T)$ using only the raw data, making no assumptions about the magnitude of $\lambda(T)$ or by imposing a theoretical temperature dependence on the data. This can be done as follows. Re-write Eq. (1), subtracting off a zero-temperature baseline from the data:

$$\ln\left\{\left(\frac{c}{v_{\text{ph}}(T)}\right)^2-\left(\frac{c}{v_{\text{ph}}(0)}\right)^2\right\} = \ln\left(\lambda(T)\coth\left(\frac{t}{\lambda(T)}\right)-\lambda(0)\coth\left(\frac{t}{\lambda(0)}\right)\right) + \ln\left(\frac{2\varepsilon_r}{d}\right)$$

The transcendental function can be eliminated from the right-hand side of this equation in the two extremes of film thickness $t>3\lambda/2$ or $t<\lambda/2$. If the additional assumption is made that the penetration depth differs only slightly from its zero temperature

value (i.e., $T < T_c/2$), then one can write

$$\ln\left\{\left(\frac{c}{v_{ph}(T)}\right)^2 - \left(\frac{c}{v_{ph}(0)}\right)^2\right\} = \ln\left(\frac{\lambda(T)}{\lambda(0)} - 1\right) + \text{const}$$

$$T < \frac{T_c}{2}; \quad \frac{t}{\lambda} < \frac{1}{2} \quad \text{or} \quad \frac{t}{\lambda} > \frac{3}{2} \qquad (2)$$

where the constant depends on $\lambda(0)$, ε_r, t, and d. The temperature dependence in this equation is solely that of the penetration depth at low temperatures.

When extrinsic effects have been eliminated, the low-temperature dependence of $\lambda(T)$ simply measures the low-lying pair-breaking excitations which deplete the density of superconducting electrons. The low-temperature dependence of presently known superconductors usually takes one of two forms [9]. For a superconductor with a finite energy gap over the entire Fermi surface, of minimum value $\Delta(0)$, the low-temperature dependence will be [10]

$$\left[\frac{\lambda(T)}{\lambda(0)} - 1\right] \alpha \frac{1}{\sqrt{T}} e^{-\Delta(0)/k_B T} \qquad (T < T_c/2)$$

In this case, a plot of the raw data in the form of Eq. (2) vs. T_c/T will be roughly a straight line of slope $-\Delta(0)/k_B T_c$. Some representative data for low-T_c and high-T_c films and the BCS theoretical prediction in the weak coupling $[2\Delta(0)/k_B T_c = 3.5]$ limit plotted in this fashion are shown in Fig. 2. (Because of the $T^{-1/2}$ prefactor, one does not expect exactly a straight line, and the theoretical points are seen to curve slightly.) The Nb data fit a line with slope $2\Delta(0)/k_B T_c \approx 3.2$, in fair agreement with the value of 3.7 found by tunneling [11].[2] However, it is clear that to the degree the data can be considered straight lines, all of the $YBa_2Cu_3O_{7-\delta}$ films show a value of $2\Delta(0)/k_B T_c < 3.5$.

Another observed low-temperature dependence for $\lambda(T)$ in superconductors is that associated with nodes in the superconducting energy gap, and has the form [9]

$$\left[\frac{\lambda(T)}{\lambda(0)} - 1\right] \alpha \left(\frac{T}{T_c}\right)^n \qquad \left(T < \frac{T_c}{2}\right)$$

To test this possibility, the data in Fig. 2 are replotted in Fig. 3 vs. $\ln(T/T_c)$ over the same temperature range. These lines are reasonably straight, and all the $YBa_2Cu_3O_{7-\delta}$ films show values of n small compared

[2]A possible explanation for this underestimate of $2\Delta(0)/k_B T_c$ is the presence of a Nb sub-oxide with $T_c = 7$ K on the surface of the film [11].

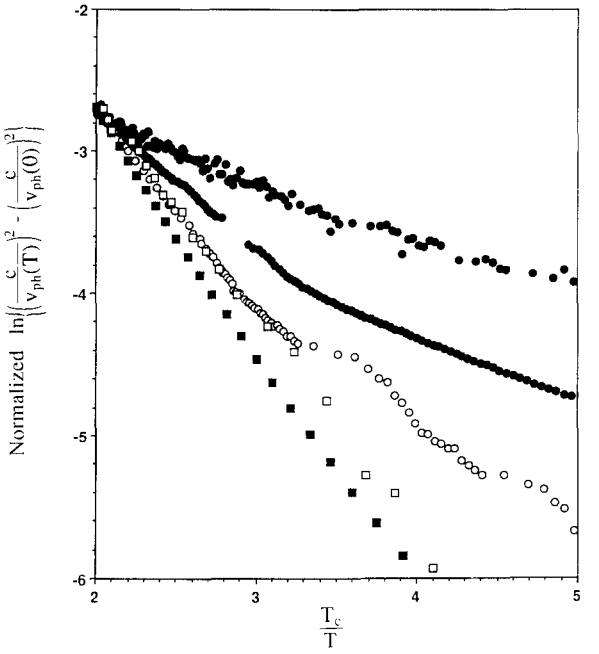

Fig. 2. Phase velocity data, with a zero-temperature baseline subtracted, plotted vs. T_c/T. Representative data from Nb (□), *in-situ* sputtered $YBa_2Cu_3O_{7-\delta}$ (●), *in-situ* coevaporated $YBa_2Cu_3O_{7-\delta}$ (○), and BCS theory (■) are presented.

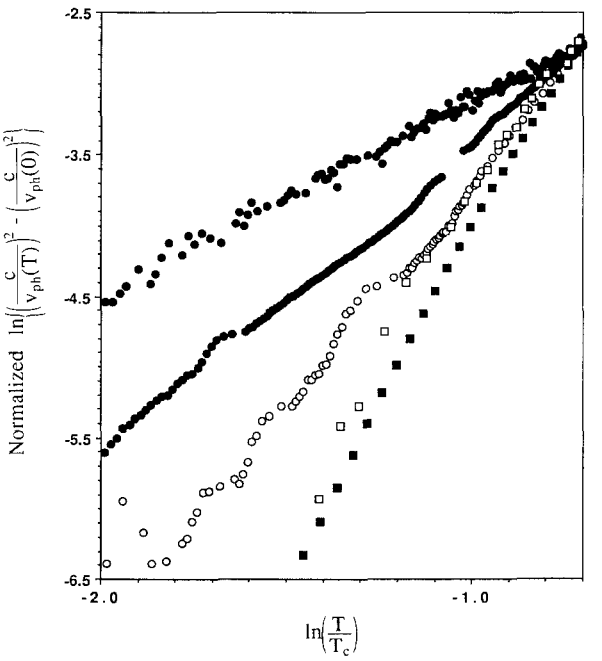

Fig. 3. Phase velocity data, with a zero-temperature baseline subtracted, plotted vs. $\ln(T/T_c)$. Representative data from Nb (□), *in-situ* sputtered $YBa_2Cu_3O_{7-\delta}$ (●), *in-situ* coevaporated $YBa_2Cu_3O_{7-\delta}$ (○), and BCS theory (■) are presented.

to the exponentially decaying weak coupled BCS theory, or the Nb film. Although both the exponential and power-law dependences describe the low-temperature data reasonably well, it is difficult to distinguish one or the other as the best. Furthermore, because of the variation in the temperature dependence of λ from film to film, we are not yet able to rule out the possibility that $\lambda(T)$ in $YBa_2Cu_3O_{7-\delta}$ is dominated by extrinsic materials properties (e.g., weak links between grains [12]).

4.2. Absolute Penetration Depth

In order to determine the absolute value of λ, we could invert the phase velocity equation [Eq. (1)] to obtain the penetration depth over the entire temperature range is we knew the effective dielectric constant of the microstrip line. However, the resulting magnitude of the penetration depth is quite sensitive to the value taken for ε_{eff}. Because there are several dielectrics in the flip-chip measurement (i.e., the substrate and dielectric sheet), it is difficult to use analytic expressions to calculate ε_{eff}, since these formulas are typically only accurate to within about 5%. In addition, obtaining ε_{eff} by measuring the characteristic impedance of the line also is inaccurate. Thus we have developed an analysis technique which allows us to obtain ε_{eff} from the phase velocity data themselves by fitting the data to an assumed penetration depth temperature dependence [13].

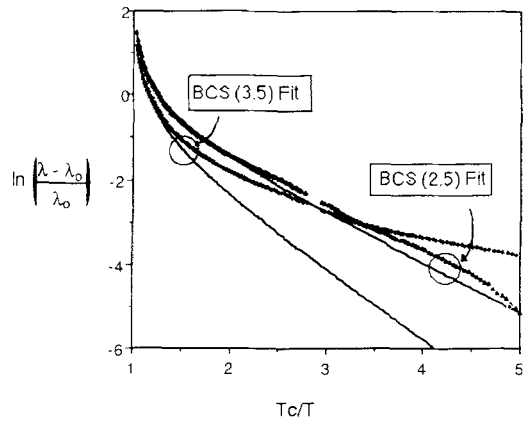

Fig. 4. Penetration depth curves, for an *in-situ* sputtered $YBa_2Cu_3O_{7-\delta}$ thin film, obtained using fits to temperature dependences calculated within the BCS framework, with $2\Delta(0)/k_BT_c$ as a parameter. The data are plotted to emphasize the exponential behavior. When the data are fitted to a BCS temperature dependence with $2\Delta(0)/k_BT_c = 3.5$, a value of $\lambda(0) = 2900$ Å is obtained. Note, however, that the analyzed data have a temperature dependence quite different from that assumed for the fit. Much better consistency is obtained when the data are fitted to a BCS dependence with $2\Delta(0)/k_BT_c = 2.5$. In that case, $\lambda(0) = 2200$ Å.

The procedure that we have developed to analyze our data is as follows. First, the data is fitted to an assumed temperature dependence calculated with BCS theory, with the T_c and the energy gap treated as fitting parameters.[3] We require that the penetration depth curve that results from the analysis have the same temperature dependence as the fit function. In general, the penetration depth of our *c*-axis normal $YBa_2Cu_3O_{7-\delta}$ films fit well to a BCS temperature dependence. However, the values of $2\Delta(0)/k_BT_c$ found for the best fit are strictly less than 3.5 for all of the films measured, consistent with the results of Section 4.1 (see Fig. 4). The values of $\lambda(0)$ for the films range from 1300 to 2000 Å.

5. CONCLUSIONS

The microstrip resonator method allows one to measure the magnetic penetration depth of thin-film superconductors with high sensitivity, particularly at low temperature. The temperature dependence of $\lambda(T)$ at low T in Nb is in good agreement with weak coupled BCS theory. For the $YBa_2Cu_3O_{7-\delta}$ films, the temperature dependence is neither clearly an exponential nor a power law. If an exponential dependence is assumed, values for $2\Delta(0)/k_BT_c$ less than 3.5 are observed. This may be consistent with a highly anisotropic energy gap if one notes that at low temperatures, one measures thermal excitation of quasiparticles only over the smallest of all energy gaps on the Fermi surface. However, the possibility remains that these temperature dependences arise from extrinsic defects in the films.

Finally, we wish to emphasize that the value of the zero-temperature penetration depth, $\lambda(0)$, depends on the form of the temperature dependence used to fit the data. We find that good fits over the entire temperature range are found for BCS temperature dependences having $2\Delta(0)/k_BT_c$ less than 3.5, consistent with our low-temperature measurements.

ACKNOWLEDGMENTS

We are indebted to J. Halbritter for many fruitful and stimulating discussions.

[3]The BCS $\lambda(T)$ is calculated by the method of J. Halbritter [14]. Parameters chosen for $YBa_2Cu_3O_{7-\delta}$ are $\xi = 15$ Å, $\lambda_L = 1400$ Å, $\ell_{\text{MFP}} = 100$ Å, and $T_c = 90$ K.

REFERENCES

1. R. E. Matick, *Transmission Lines for Digital and Communication Networks*, (McGraw-Hill, New York, 1969), p. 243.
2. K. Chang, *J. Appl. Phys.* **50**, 8129 (1979).
3. S. M. Anlage, B. W. Langley, and M. R. Beasley, submitted to *Rev. Sci. Inst.*
4. S. I. Park, Ph.D. Thesis, Stanford University, 1986.
5. C. B. Eom, J. Z. Sun, K. Yamamoto, A. F. Marshall, K. E. Luther, T. H. Geballe, and S. S. Laderman, *Appl. Phys. Lett.* **55**, 595 (1989).
6. N. Missert, R. Hammond, J. E. Mooij, V. Matijasevic, P. Rosenthal, T. H. Geballe, A. Kapitulnik, M. R. Beasley, S. S. Laderman, C. Lu, E. Garwin, and R. Barton, *IEEE Trans. Magn.* **MAG-25**, 2418 (1989); V. Matijasevic, P. Rosenthal, K. Shinohara, R. H. Hammond, A. Marshall, and M. R. Beasley, *Bull. Am. Phys. Soc.* **35**, 383 (1990).
7. S. Tahara, S. M. Anlage, J. Halbritter, C. B. Eom, D. K. Fork, T. H. Geballe, and M. R. Beasley, *Phys. Rev. B* **41**, 11203 (1990).
8. C. B. Eom, J. Z. Sun, S. K. Streiffer, A. F. Marshall, K. Yamamoto, B. M. Lairson, S. M. Anlage, S. S. Laderman, R. Taber, and T. H. Geballe, submitted to *Phys. Rev. B.*
9. J. F. Annett, N. Goldenfeld, and S. R. Renn, preprint; N. Goldenfeld, S. R. Renn, and J. F. Annett, *Bull. Am. Phys. Soc.* **35**, 785 (1990).
10. J. Halbritter, *Z. Phys.* **243**, 201 (1971).
11. R. F. Broom and P. Wolf, *Phys. Rev. B* **16**, 3100 (1977); J. Halbritter, *J. Appl. Phys.* **46**, 1403 (1975).
12. T. L. Hylton and M. R. Beasley, *Phys. Rev. B* **39**, 9042 (1989).
13. S. M. Anlage, H. Sze, H. J. Snortland, S. Tahara, B. Langley, C. B. Eom, M. R. Beasley, and R. Taber, *Appl. Phys. Lett.* **54**, 2710 (1989); B. W. Langley, S. M. Anlage, J. Halbritter, N. Switz, M. R. Beasley, and R. F. W. Pease, *Bull. Am. Phys. Soc.* **35**, 786 (1990).
14. J. Halbritter, *Z. Phys.* **266**, 209 (1974).